



Sestrin2 balances mitophagy and apoptosis through the PINK1-Parkin pathway to attenuate severe acute pancreatitis

Yuxi Yang, Yiqiu Peng, Yingying Li, Tingjuan Shi, Ning Xu, Yingyi Luan^{*}, Chenghong Yin^{*}

Department of Central Laboratory, Beijing Obstetrics and Gynecology Hospital, Capital Medical University, Beijing Maternal and Child Health Care Hospital, Beijing 100026, China

ARTICLE INFO

Keywords:
severe acute pancreatitis
mitophagy
sestrin2
monocyte macrophage
apoptosis

ABSTRACT

Mitophagy serves as a mitochondrial quality control mechanism to maintain the homeostasis of mitochondria and the intracellular environment. Studies have shown that there is a close relationship between mitophagy and apoptosis. Sestrin2 (Sesn2) is a highly conserved class of stress-inducible proteins that play important roles in reducing oxidative stress damage, inflammation, and apoptosis. However, the potential mechanism of how Sesn2 regulates mitophagy and apoptosis in severe acute pancreatitis (SAP) remains unclear. In the study, RAW264.7 (macrophage cell line) cellular inflammation model established by lipopolysaccharide (LPS) treatment as well as LPS and CAE-induced SAP mouse model (wild-type and Sesn2 Knockout mouse) were used. Our study showed that LPS stimulation significantly increased the level of Sesn2 in RAW264.7 cells, Sesn2 increased mitochondrial membrane potential, decreased inflammation levels, mitochondrial superoxide levels and apoptosis, and also promoted monocyte macrophages toward the M2 anti-inflammatory phenotype, suggesting a protective effect of Sesn2 on mitochondria. Further, Sesn2 increased mitophagy and decreased apoptosis via modulating the PINK1-Parkin signaling. Meanwhile, knockout of Sesn2 exacerbated pancreatic, mitochondrial damage and inflammation in a mouse model of SAP. In addition, the protective effect of Sesn2 against SAP was shown to be associated with mitophagy conducted by the PINK1-Parkin pathway via inhibiting apoptosis. These findings reveal that Sesn2 in balancing mitochondrial autophagy and apoptosis by modulating the PINK1-Parkin signaling may present a new therapeutic strategy for the treatment of SAP.

1. Introduction

Acute pancreatitis (AP) is an inflammatory disease associated with pancreatic exocrine tissue injury and necrosis. It has a rapid onset and poor prognosis, as it can damage important parenchymal organs such as the lungs, kidneys, liver, and heart to varying degrees [1,2]. Overall, the global annual incidence of AP is 34 cases per 100,000 people, with a mortality rate of about 1%–5% [3]. When AP progresses to persistent organ failure (>48 h), it is called severe acute pancreatitis (SAP) [4]. A growing body of research indicates that macrophages mediate systemic inflammatory processes during SAP development [5,6]. The currently recognized pathogenesis of SAP involves mitochondrial dysfunction due to the altered mitochondrial membrane potential (MMP) [7–10].

Mitochondrial dysfunction occurs in various models of pancreatitis, resulting in the loss of MMP and mitochondrial fracture [11,12]. Most of the current treatments for SAP involve conservative methods such as nutritional support and fluid management. Due to the lack of specific molecular targets, the treatment of SAP remains a considerable challenge [13–15].

Mitochondria are cellular energy centers present in most eukaryotic cells, where they perform aerobic respiration and produce adenosine triphosphate (ATP) through oxidative phosphorylation. Conditions such as cardiovascular disease, metabolic disease, inflammatory disease, or cancer damage mitochondria, leading to mitochondrial dysfunction. Mitophagy is a process that eliminates damaged mitochondria to maintain homeostasis in the body [16,17]. It is subdivided into two

Abbreviations: SAP, Severe acute pancreatitis; Sesn2, Sestrin2; Hi95, Hypoxia-inducible gene 95; ATP, Adenosine Triphosphate; LPS, Lipopolysaccharide; ROS, Reactive oxygen species; AMPK, AMP-Activated Protein Kinase; OMM, outer mitochondrial membrane; Ub, Ubiquitin; TOM, Translocase of outer mitochondrial membrane; TEM, Transmission electron microscopy; MitoSOX, Mitochondrial superoxide; Arg-1, arginase-1.

^{*} Corresponding authors at: Beijing Obstetrics and Gynecology Hospital, Capital Medical University, Beijing Maternal and Child Health Care Hospital, Beijing 100026, China.

E-mail addresses: luanyingyi@mail.ccmu.edu.cn (Y. Luan), yinchh@ccmu.edu.cn (C. Yin).

<https://doi.org/10.1016/j.cellsig.2024.111518>

Received 27 June 2024; Received in revised form 8 September 2024; Accepted 18 November 2024

Available online 20 November 2024

0898-6568/© 2024 The Authors. Published by Elsevier Inc. This is an open access article under the CC BY-NC-ND license (<http://creativecommons.org/licenses/by-nc-nd/4.0/>).

categories: ubiquitin (Ub)-dependent pathways and Ub-independent pathways [18]. Ub-independent pathways refer to several autophagy receptors on the outer mitochondrial membrane (OMM), which can bind to LC3 without ubiquitylation to initiate mitophagy [19]. Another pathway called the PTEN-induced putative kinase 1 (PINK1)/Parkin pathway is the most extensively studied. PINK1 accumulates at the OMM via the translocase of the outer mitochondrial membrane (TOM), which activates and recruits Parkin, after which the subsequent ubiquitination of proteins on the OMM by Parkin induces mitophagy [20]. Mitophagy plays a protective role in cardiovascular diseases, metabolic diseases, and neurodegenerative diseases [21,22]. However, it remains unclear whether mitophagy is involved in the process of SAP, which is vital for the targeted treatment of SAP.

Sestrins are a highly conserved family of stress-inducible proteins. Sestrin2 (Sesn2), also known as the hypoxia-inducible gene 95 (Hi95). Sesn2 may be associated with hypoxia, endoplasmic reticulum stress, oxidative stress, starvation, and DNA damage [23,24]. Sesn2 has been the most studied isoform of sestrin over the years. Besides its ability to reduce oxidative stress damage and protect cells, it can also inhibit the mechanistic target of rapamycin complex 1 (mTORC1) through AMP-activated protein kinase (AMPK)-dependent or independent pathways, thereby exerting cytoprotective functions in organs such as the heart, lungs, and liver [25]. Sesn2 is also a promising therapeutic target in metabolic diseases, hypoxia-related diseases, cardiovascular diseases, and cancer [26–28]. The potential role of Sesn2 in macrophages has been increasingly recognized, with it being demonstrated to decrease the generation of oxidized low-density lipoprotein-induced reactive oxygen species (ROS) and apoptosis in RAW264.7 cells [29]. Currently, no studies have found an association of Sesn2 and SAP and whether Sesn2 is involved in regulating the expression of macrophage mitophagy in SAP.

This study aimed to investigate how Sesn2 mediates the disease process of SAP. Our data demonstrated that knockout of Sesn2 aggravated the impairment of pancreatic function and mitochondrial dysfunction in SAP mice. Mechanistically, Sesn2 enhanced mitophagy by regulating the PINK1-Parkin pathway, reduces mitochondrial damage and inflammation levels, thereby attenuating apoptosis, formation of ROS and inflammation, as well as increasing the MMP. It also promoted the differentiation of macrophage toward the M2 phenotype. These findings suggest that Sesn2 may be a therapeutic target for preventing the progression of SAP.

2. Materials and methods

2.1. Materials

Ceruletide (CAE) was purchased from AbMole (M9316), and lipopolysaccharide (LPS; from *E. coli* O111: B4) was obtained from Sigma (L2630). DMEM medium was purchased from Gibco (C11995500BT) and Mdivi-1 was purchased from MedChemExpress (HY-15886). Sqstm1/p62 (ab109012), Sesn2 (ab178518), BAX (ab32503), Bcl-2 (ab182858), Beclin1 (ab207612), iNOS (ab178945), and TOMM20 (ab186735) were obtained from Abcam. Goat anti-mouse IgG H&L (Alexa Fluor® 647) and goat anti-rabbit IgG H&L (Alexa Fluor® 488) were also obtained from Abcam (ab15007, ab150115). Mouse anti-β actin mAb (TA-09), horseradish peroxidase-labeled goat anti-mouse IgG H&L (ZB2305) and horseradish peroxidase-labeled goat anti-rabbit IgG H&L (AB-2301) were purchased from ZSGB-BIO. PINK1 (23274-1-AP) and Parkin (14060-1-AP) antibodies were obtained from Proteintech. Cleaved caspase3 (9661S), Arg-1 (93668), and LC3A/B (4108) were all purchased from Cell Signaling Technology.

2.2. Animal experiments

Specific pathogen-free (SPF) wild-type (WT) C57BL/6 J mice were purchased from Beijing Vital River Laboratory Animal Technology Co.

Sesn2 knockout (Sesn2^{-/-}) mice with C57BL/6 J background were obtained from the Gempharmatech Co. (Jiangsu, China). The Sesn2 gene exon 3–6 was knocked out using the CRISPR/Cas9 technique and a Sesn2 knockout mouse model was established. Expert reports on the knockout effects are provided as Supplementary Information. Briefly, 8-week-old male C57BL/6 J mice weighing 20–25 g were kept in aseptic conditions at the Laboratory Animal Center, at a room temperature of 20–25 °C, relative humidity of 40 %–50 %, and a photoperiod of 12 h to acclimatize to the environment for 1 week. The animals were given unrestricted access to aseptic feed and water. To induce SAP, WT or Sesn2^{-/-} mice were fasted for 12 h before the experiment, then injected intraperitoneally with 100 µg/kg CAE once an hour for seven times. After the last CAE injection, 10 mg/kg LPS was injected intraperitoneally. Serum, primary monocyte macrophages, and pancreas and lung tissues were collected 24 h after modeling.

Histopathological analysis.

Fresh tissues were fixed in 4 % paraformaldehyde for over 24 h, dehydrated, and embedded for paraffin sectioning. Then, the sections were sequentially transferred to an ethanol solution with different concentrations for dehydration. Then, wash the slices with distilled water. The nucleus was stained using hematoxylin and the cytoplasm was stained using eosin (G1120, Solarbio). The sections were then dehydrated and sealed with neutral tree glue. The images were observed under a light microscope (Nikon Eclipse CI, Japan). The degree of pathological damage to the pancreas was scored.

2.3. Western blot assay

Proteins were extracted from the pancreatic tissue and RAW264.7 cells using RIPA lysis buffer (R0020, Solarbio). Protein concentrations in the cell and tissue were measured using the BCA protein assay kit (P0010, Beyotime Biotechnology). The protein samples at equal concentrations were separated on an SDS-PAGE gel, and the resolved proteins were transferred onto a 0.45 µm PVDF membrane (IPVH00010, Millipore). After the transfer was complete, the membrane was incubated in 5 % skimmed milk for 2 h, and then with the primary antibodies at 4 °C overnight. Primary antibodies Parkin, PINK1, Sesn2, LC3A/B, BAX, Cleaved caspase3, TOMM20, iNOS and Arg-1 were diluted at a ratio of 1:1000; Bcl-2, Beclin 1 and β-actin were diluted at a ratio of 1:2000; Sqstm1/p62 was diluted at a ratio of 1: 10000. After this, the appropriate secondary antibody (ZSGB-BIO, China) was selected according to the primary antibody source of the target protein and then incubated in a shaker at room temperature for 1 h. Finally, the image of the target protein was analyzed using the Immobilon Chemilum Western HRP Substrate (WBKLS0500, Millipore).

2.4. Immunofluorescence and immunohistochemical staining

The prepared cells were fixed with 4 % paraformaldehyde for 30 min and washed 3 times with PBS (P1020, Solarbio), and then permeabilized with 0.3 % Triton X-100 (T8200, Solarbio) at room temperature for 10 min. The cells were sealed by adding 5 % BSA (A8010, Solarbio) dropwise at room temperature for 1 h. The primary antibody was diluted proportionally according to the manufacturer's instructions, added dropwise to the slide, incubated at 4 °C overnight, and stored at room temperature away from light. The unbound primary antibody was then removed by washing thrice with PBS, after which the secondary antibody was added and incubated at room temperature in the dark for 60 min. The antibody-treated cells were visualized under a fluorescence microscope. Finally, an anti-fluorescence burst sealer (ZLI-9557, ZSGB-BIO) was added and the cells were observed under a fluorescence microscope (MICA, Leica).

Pancreatic tissues were fixed for 48 h at 4 °C in 4 % paraformaldehyde. Fixed samples were washed with water, dehydrated in gradient ethanol, cleared in xylene, embedded in paraffin wax at 52–54 °C, and sliced into sections of 4–10 µm thickness. Antigen repair

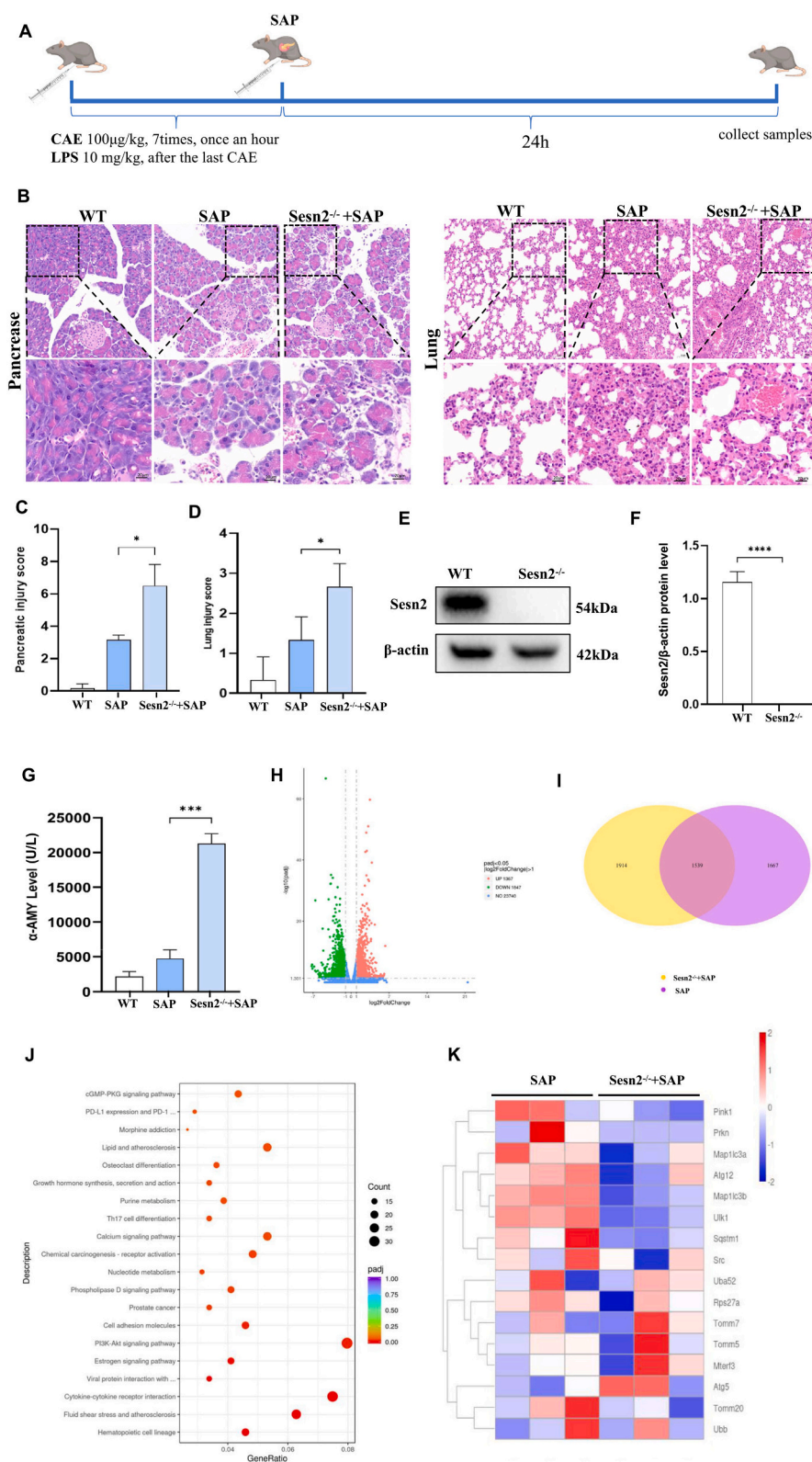


Fig. 1. Knockout of SESN2 aggravates pancreatic impairment in SAP mice induced by LPS and CAE.

A: Flowchart for constructing the animal model of SAP. Wild-type and *Sesn2*^{-/-} mice were injected with CAE and LPS (*n* = 6/group). **B:** HE staining was used to observe injury to the pancreas and lungs. **C-D:** Injury score of pancreas and lungs. **E-F:** Results of Western blotting (**E**) and densitometric quantification (**F**) of *Sesn2* in wild-type and *Sesn2*^{-/-} mice. **G:** Serum α -AMY levels in various groups of mice (*n* = 6/group). RNA-seq data analysis from SAP and *Sesn2*^{-/-} + SAP mice. **H:** Volcano plot analysis of DEGs. **I:** Venn diagram analysis of the DEGs. **J:** KEGG pathway analysis of the DEGs. **K:** Heatmap of DEGs in the mitophagy pathway. **P* < 0.05, ****P* < 0.001, *****P* < 0.0001. CAE, ceruletide; DEGs, differentially expressed genes; LPS, lipopolysaccharide; SAP, severe acute pancreatitis.

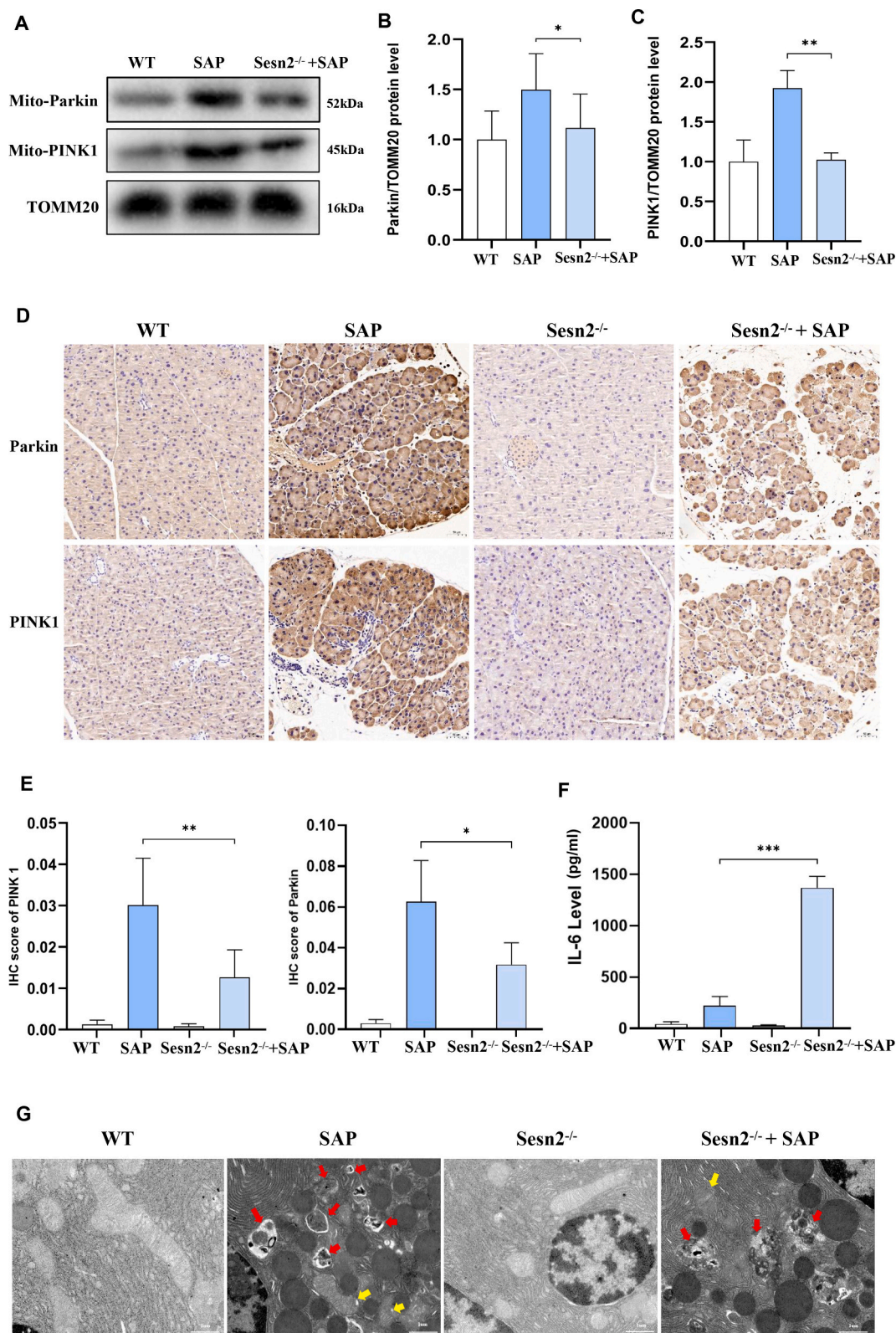


Fig. 2. Promotion of PINK1-Parkin-mediated mitophagy by Sesn2 attenuates mitochondrial dysfunction and inflammation levels in SAP mice. WT and Sesn2^{-/-} mice were injected with CAE and LPS (n = 6/group). **A-C:** Results of Western blotting (**A**) and densitometric quantification of Mito-Parkin (**B**) and Mito-PINK1 (**C**) mitochondrial proteins in mouse pancreatic tissue from different groups. **D-E:** Representative images (**D**) and statistical graphs (**E**) for Parkin and PINK1 immunohistochemical staining (Bar = 50 μm). **F:** Results of ELISA of serum IL-6 level in various groups of mice (n = 6/group). **G:** Representative TEM images of mitochondrial autophagosomes and autophagosomes (red arrowheads) and mitochondrial damage (yellow arrowheads) in pancreatic tissues from different groups (Bar = 1 μm). **P* < 0.05, ***P* < 0.01, ****P* < 0.001. CAE, ceruletide; LPS, lipopolysaccharide; PINK1, PTEN-induced putative kinase 1; TEM, transmission electron microscopy. (For interpretation of the references to colour in this figure legend, the reader is referred to the web version of this article.)

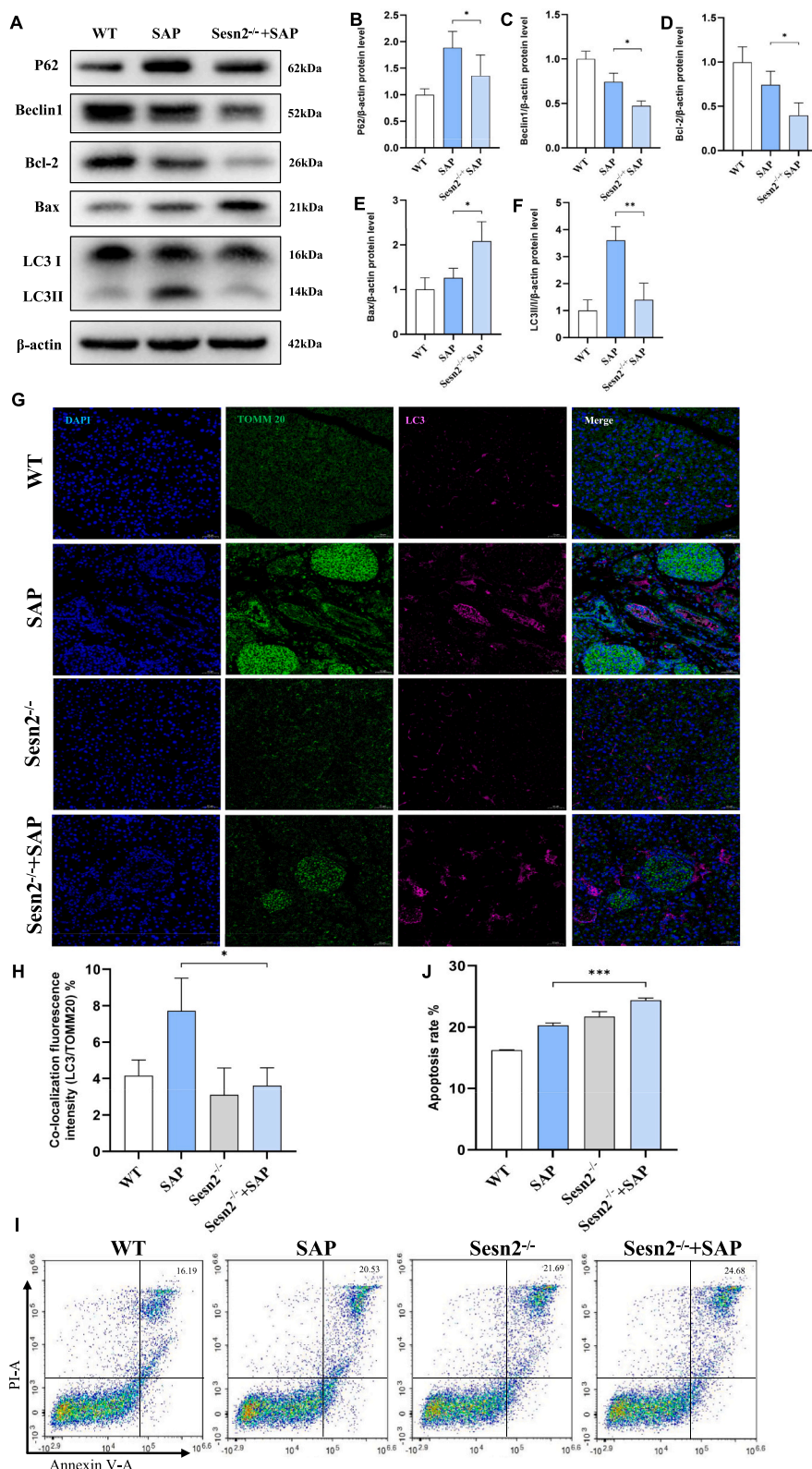


Fig. 3. Sesn2 attenuates apoptosis by enhancing mitophagy in SAP mice. WT and Sesn2^{-/-} mice were injected with CAE and LPS (n = 6/group). **A–F:** Results of Western blotting (**A**) and densitometric quantification (**B–F**) of Sqstm1/p62, Beclin1, Bcl-2, Bax, and LC3II/I in different groups. **G–H:** Co-localization (**G**) and mean Co-localization fluorescence intensity analyses (**H**) of LC3 (red) with TOMM20 (green) in mouse pancreatic tissue from different groups. **I–J:** Flow cytometry (**I**) and apoptosis ratio analyses (**J**) were used to detect apoptosis of primary monocyte macrophages in mice of each group. **P* < 0.05, ***P* < 0.01, ****P* < 0.001. CAE, ceruletide; LPS, lipopolysaccharide; PINK1, PTEN-induced putative kinase 1. (For interpretation of the references to colour in this figure legend, the reader is referred to the web version of this article.)

was performed with a sodium citrate antigen repair solution, followed by permeabilization with 0.02 % Triton-100 for 40 min. The samples were blocked with 5 % BSA for 1 h at room temperature, followed by incubation with primary antibody at 4 °C overnight and secondary antibody at 37 °C for 30 min. Finally, the DAPI-containing sealer (ZLI-9557, ZSGB-BIO) was added dropwise to the pancreatic tissue. Under a fluorescence microscope, the images were observed and photographed. The obtained images were analyzed using the Image J software.

2.5. Transmission electron microscopy (TEM)

First, 1–3 mm³ of pancreatic tissue was taken and immersed in 2.5 % glutaraldehyde. Then 1 % osmic acid prepared with 0.1 M phosphate buffer (PB, pH 7.4) was fixed in darkness at room temperature for 2 h. Then, the tissue was rinsed thrice in 0.1 M PB (pH 7.4) for 15 min each time. After dehydration using ethanol at room temperature and embedding in acetone, the sections were stained with 2 % uranyl acetate-saturated alcohol solution in the dark and 2.6 % lead citrate solution avoiding carbon dioxide. Observations and photographs were taken under a transmission electron microscope (FT7800, Hitachi) and images were collected for analysis.

The sections were observed and photographed under a transmission electron microscope (FT7800, Hitachi) and images were collected for analysis.

2.6. Cell culture

Mouse monocyte-macrophage leukemia cells (RAW264.7) were purchased from Pricella (Cat. No. CL-0190). The cells were cultivated in DMEM medium with 10 % FBS (Sigma) and 1 % penicillin and streptomycin (Gibco) in a constant-temperature incubator at 37 °C with 5 % CO₂. Care was taken to ensure no contamination with human progenitor cells or mycoplasma. After cell adhesion, 10 μM Mdivi-1 was added one hour before the addition of 1 μg/mL LPS and co-cultured for 24 h. Subsequently, cellular proteins were extracted for western blot analysis, while inflammatory cytokines in the culture medium supernatant were detected.

2.7. Transfection with small-interfering RNA (siRNA)

To inhibit the expression of *Sesn2*, RAW264.7 cells were transfected with siRNAs targeting *Sesn2* (GCAUCAGAUACGAUGACUATT), while the control group was transfected with NC-siRNA, both of which were obtained from Ribobio (Shanghai, China). The cells were then transfected using jetPRIME transfection reagents (Polyplus, French). Cellular proteins were extracted after 48 h of culture and the efficiency of knockdown was assessed using the Western blot (WB) assay.

2.8. Extraction of mitochondrial proteins

Cellular mitochondrial proteins were extracted from the RAW264.7 cells using the cellular mitochondrial isolation kit (C3601, Beyotime). Tissue mitochondrial protein was extracted from the mouse pancreas using the tissue mitochondrial isolation kit (C3606, Beyotime).

2.9. Flow cytometry

To detect apoptosis in different groups of cells, an apoptosis detection kit (C1062L, Beyotime) was used. The cells were collected and subjected to flow cytometry; annexin V-FITC for green fluorescence and propidium iodide (PI) for red fluorescence.

To detect the M1M2 typing of the RAW264.7 cells, the collected cells (5–10 × 10⁶ cells/mL) were assayed using flow cytometry by adding the fluorescently labeled antibodies APC anti-mouse CD206 (141,707, Biolegend) and PE/Cyanine7 anti-mouse CD86 (1,050,137, Biolegend).

2.10. Detection of ROS

DCFH-DA (S0033S, Beyotime) was diluted 1:1000 in serum-free culture medium. Cells were harvested, suspended in diluted DCFH-DA and incubated in a cell incubator at 37 °C for 20 min. Cells were washed thrice with a serum-free cell culture medium. Finally, ROS levels were detected using flow cytometry.

The cells were stimulated using the mitochondrial superoxide indicator MitoSOX Red (M36008, Invitrogen) in combination with Hoechst (C1022, Beyotime) staining, followed by laser confocal photography, and the level of mitochondrial superoxide was determined based on the intensity of red fluorescence.

2.11. Determination of MMP

The MMP assay kit (JC-1) (C2006, Beyotime) was used for this purpose. First, 1 mL of JC-1 staining working solution was prepared and mixed well. The cells were then incubated for 20 min at 37 °C in a cell incubator. The supernatant was aspirated and washed twice with 1 × JC-1 staining buffer. Finally, cell cultures was added and the MMP was examined under a laser confocal microscope.

Mito-Tracker Red CMXRos (C1035, Beyotime) was used as an indicator probe to determine the MMP. Mito-Tracker Red CMXRos working solution was first added and incubated at 37 °C for 30 min, after which the nuclei were stained with Hoechst. Then, the Mito-Tracker Red CMXRos working solution was removed and the culture medium was added. The solution was then observed under a laser confocal microscope.

2.12. ELISA assay

The collected cell supernatants and mouse sera were assayed using ELISA kits (EK282, EK210, and EK206; Multi Sciences) to determine the levels of IL-6, IL-10, and TNF-α. The OD₄₅₀ values were determined using an enzyme marker. The final concentration was calculated from the obtained OD₄₅₀ values.

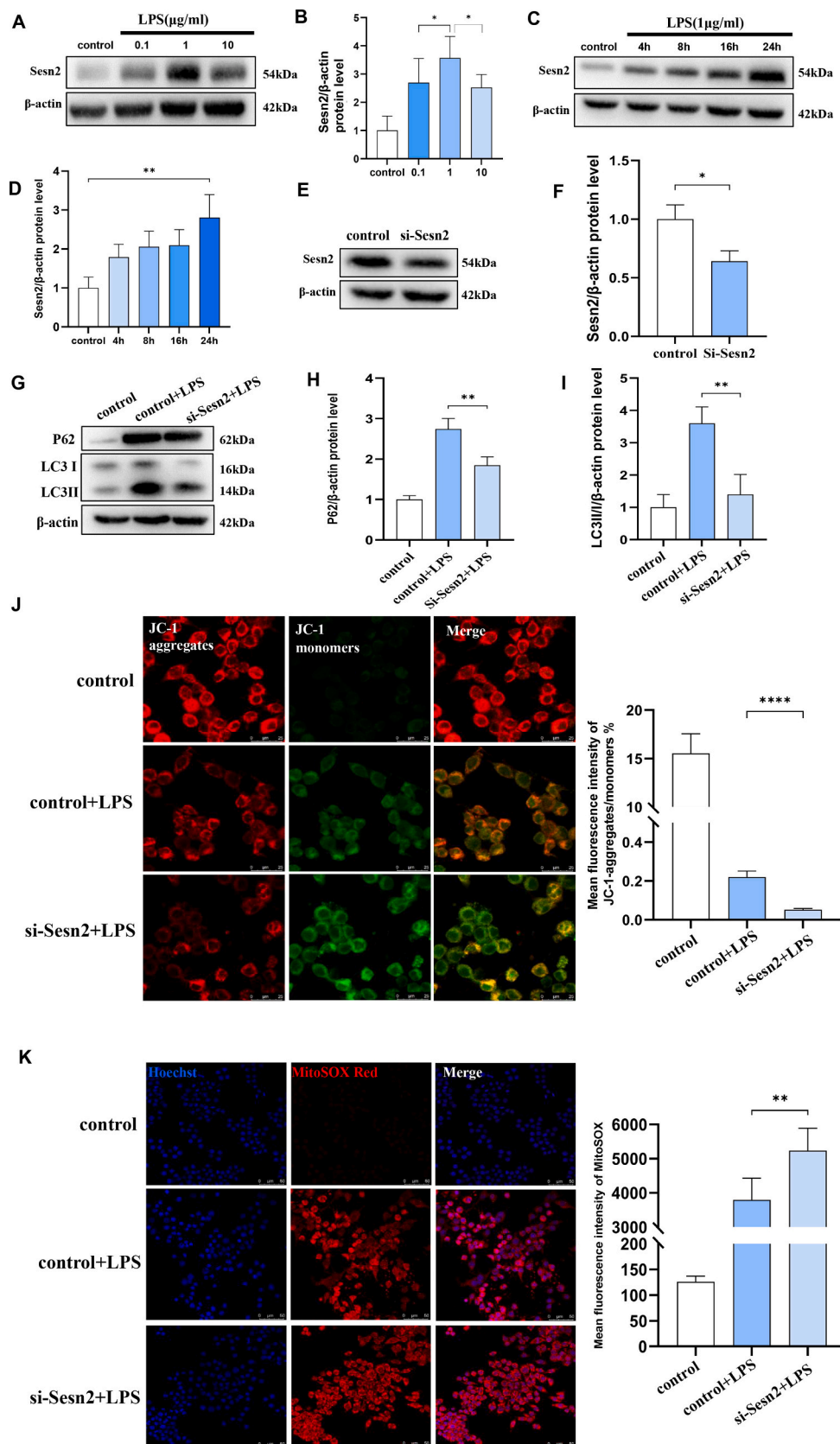
2.13. Statistical analysis

The statistical analysis was performed using the statistical software GraphPad Prism version 9.0. Data were expressed as mean ± Standard Deviation (SD). Two independent groups were compared using a two-sided *t*-test, while more than two groups were compared using one-way ANOVA combined with Tukey's post-hoc test. *P*-values of <0.05 indicated statistically significant differences. * *P* < 0.05, ** *P* < 0.01, *** *P* < 0.001, and **** *P* < 0.0001.

3. Results

3.1. Knockout of *SESN2* aggravates pancreatic impairment in SAP mice induced by LPS and CAE

For the preliminary assessment of the potential role of *Sesn2* in SAP, we injected WT mice and *Sesn2* knockout (*Sesn2*^{-/-}) mice with LPS and CAE to establish the SAP model. We injected 100 μg/kg CAE intraperitoneally once an hour for seven times and 10 mg/kg LPS after the last CAE injection. Samples were collected 24 h after the last injection (Fig. 1A). HE staining (Fig. 1B, C) indicated that in the *Sesn2*^{-/-} + SAP group, the pancreatic tissue structure was severely abnormal with several necrotic follicular cells, the nuclei of the cells were fixed and deeply stained and several inflammatory cells infiltrated in the tissue. The pancreatic injury scores of the *Sesn2*^{-/-} + SAP group were significantly higher compared with SAP group, suggesting that the knockout of *Sesn2* could have aggravated the pancreatic injury. HE staining of the lungs also demonstrated that bronchial lumen hemorrhage and a large number of inflammatory cells infiltrated the tissues of *Sesn2*^{-/-} + SAP



(caption on next page)

Fig. 4. Inhibition of *Sesn2* decreases the MMP of RAW264.7 cells, increasing ROS levels.

A–B: RAW264.7 cells were stimulated using 0, 0.1, 1, and 10 $\mu\text{g}/\text{mL}$ LPS. Western blot results (A) and densitometric quantification (B) of *Sesn2* expression. **C–D:** RAW264.7 cells were stimulated with 1 $\mu\text{g}/\text{mL}$ LPS for 0, 4, 8, 16, and 24 h, respectively. Western blot results (C) and densitometric quantification (D) of *Sesn2* expression. **E–F:** RAW264.7 cells were transfected with Si-*Sesn2* for 24 h before LPS stimulation to validate the constructed transfection model. Western blot results (E) and densitometric quantification (F) of *Sesn2* expression. **G–I:** Western blotting results (G) and densitometric quantification (H–I) of *Sqstm1/p62* and *LC3II/I* in different groups. **J:** MMP assay kit (JC-1) was used to detect and quantify MMP. Red fluorescence indicates JC-1 aggregates, green fluorescence indicates JC-1 monomers (Bar = 25 μm). **K:** Analysis of mitochondrial superoxide and mean fluorescence intensity. Red fluorescence indicates Mito-Tracker and blue fluorescence indicates Hoechst (Bar = 50 μm). * $P < 0.05$, ** $P < 0.01$ and **** $P < 0.0001$. LPS, lipopolysaccharide; MMP, mitochondrial membrane potential; ROS, reactive oxygen species. (For interpretation of the references to colour in this figure legend, the reader is referred to the web version of this article.)

group mice, suggesting that the knockout of *Sesn2* may have further exacerbated the systemic organ injury in SAP (Fig. 1D). The results of the WB analysis confirmed the knockout efficiency of *Sesn2* (Fig. 1E, F). α -Amylas (α -AMY) can be used as a diagnostic tool for AP. Measurement of serum samples from the three groups of mice revealed that α -AMY levels were significantly elevated in the *Sesn2*^{-/-} + SAP group compare with SAP group, confirming the findings of HE staining (Fig. 1G).

To further investigate how *Sesn2* regulates LPS and CAE-induced pancreatic injury and SAP progression, we performed transcriptomic analyses of SAP and *Sesn2*^{-/-} + SAP mice. RNA sequencing (RNA-seq) identified 1367 upregulated genes and 1847 downregulated genes, with a log₂ fold change of >1 and a *P* value of <0.05 (Fig. 1H). The Venn diagrams in Fig. 1I present differentially expressed genes appearing in the two groups. KEGG pathway analysis of the RNAseq data revealed that *Sesn2*^{-/-} + SAP mice were significantly associated with cytokine-cytokine receptor interaction, nucleotide metabolism, and other pathways compared with SAP mice (Fig. 1J). The heatmap showed that the expression of the genes *PINK1*, *Parkin*, *LC3*, and *Sqstm1/p62*, which are associated with the induction of mitophagy, was downregulated in *Sesn2*^{-/-} + SAP mice (Fig. 1K).

3.2. Promotion of *PINK1*-*Parkin*-mediated mitophagy by *Sesn2* attenuates mitochondrial dysfunction and inflammation levels in SAP mice

WB analysis was performed to further explore the role of *Sesn2* and mitophagy in SAP, which confirmed that the mitochondrial protein levels of *PINK1* and *Parkin* were decreased in the pancreatic tissues of *Sesn2*^{-/-} + SAP mice compared with SAP mice (Fig. 2A–C). Consistent with this finding, immunohistochemistry (IHC) analysis showed that the IHC scores of mitophagy-associated proteins *PINK1* and *Parkin* were significantly decreased in the pancreatic tissues of *Sesn2*^{-/-} + SAP mice compared with SAP mice, suggesting that *Sesn2* was associated with mitophagy and could promote it (Fig. 2D, E). We then examined the serum levels of the pro-inflammatory factor IL-6 in mice and showed that the knockout of *Sesn2* elevated the levels of IL-6 (Fig. 2F). Next, we examined the mitochondrial damage, lysosomes, mitochondrial autophagosomes and autophagosomes in WT, SAP, *Sesn2*^{-/-}, and *Sesn2*^{-/-} + SAP mice by electron microscopy. In SAP group, the mitochondria were mildly swollen, most of the cristae were broken off and dissolved, and the membrane structure was partly blurred (yellow arrows), with an abundance of zymogen granules and abundant mitochondrial autophagosomes, autolysosomes, and autophagosomes (red arrowheads). In contrast, the *Sesn2*^{-/-} + SAP group showed severe mitochondrial swelling with extensive mitochondrial cristae dissolution and disappearance (yellow arrow), while few autolysosomes and autophagosomes (red arrowheads). This indicated that the knockout of *Sesn2* aggravated the damage to the mitochondrial structure and reduced mitophagy (Fig. 2G).

3.3. *Sesn2* attenuates apoptosis by enhancing mitophagy in SAP mice

Mitochondrial dysfunction occurs in various models of pancreatitis and is mainly characterized by the loss of MMP and mitochondrial fragmentation. Mitophagy is necessary to remove dysfunctional mitochondria, and damaged mitochondria can inhibit apoptosis through mitophagy, which is involved in the repair of pancreatic injury [30]. WB

assays demonstrated that the expression levels of mitophagy-related proteins *Sqstm1/p62*, *Beclin1*, *Bcl-2*, and *LC3I/II* were significantly decreased, whereas the expression of the apoptotic protein *Bax* was significantly increased in the pancreatic tissues of mice following knockout of *Sesn2*. This confirms that the knockout of *Sesn2* increases apoptosis and decreases autophagy levels (Fig. 3A–F). To further confirm the relationship between *Sesn2* and mitophagy in SAP mice, we performed fluorescent staining of *LC3* and the mitochondrial marker *TOMM20* and observed that the co-localization of *LC3* with *TOMM20* was reduced in *Sesn2*^{-/-} + SAP mice compared with SAP mice (Fig. 3G–H). Moreover, we extracted primary monocyte macrophages from the spleen of mice and examined the levels of apoptosis in the four groups of mice. We observed that the degree of apoptosis in mice in the *Sesn2*^{-/-} + SAP group was significantly higher than that in mice in the SAP group (Fig. 3I, J). These results collectively suggest that *Sesn2* attenuates apoptosis by enhancing the *PINK1*-*Parkin*-mediated mitophagy.

3.4. Inhibition of *Sesn2* decreases the MMP of RAW264.7 cells, thus increasing ROS levels

For the in vitro experiments, the inflammation model of RAW264.7 cells was established by LPS treatment, we stimulated RAW264.7 cells with different concentrations of LPS. WB assay analysis showed that the expression of *Sesn2* was the highest when stimulated with 1 $\mu\text{g}/\text{mL}$ LPS (Fig. 4A, B). Next, to explore the optimal time for LPS stimulation, we stimulated the RAW264.7 cells with 1 $\mu\text{g}/\text{mL}$ LPS for 0, 4, 8, 16, and 24 h, and observed that the cellular *Sesn2* expression was the highest at 24 h of stimulation (Fig. 4C, D). Transfection of RAW264.7 cells with *Sesn2*-targeted siRNA resulted in a significant decrease in the protein level of *Sesn2*, indicating successful transfection (Fig. 4E, F). Subsequently, we examined the expression levels of autophagy-related proteins in the *Sesn2* knockdown (Si-*Sesn2*) cells. Following stimulation of RAW264.7 cells and Si-*Sesn2* cells with LPS, WB analysis revealed that knockdown of *Sesn2* decreased the levels of *Sqstm1/p62* and *LC3I/II* proteins compared with control + LPS group. This indicated that *Sesn2* could increase the expression of autophagy-related proteins, thereby promoting autophagy (Fig. 4G–I).

A decrease in the MMP is a hallmark event in the early stage of apoptosis. To detect the MMP of each group of cells, JC-1 was used as a fluorescent probe. When the MMP is high, JC-1 accumulates in the matrix of the mitochondria and forms a polymer (JC1-aggregates), which can produce red fluorescence. When the MMP is low, JC-1 cannot accumulate in the matrix of the mitochondria, and JC-1 is a monomer JC1-monomers, which can produce green fluorescence. Therefore, Fig. 4J quantifies the MMP using JC1-aggregates/monomers and it was observed that the JC1-aggregates/monomers ratio was lowest in the Si-*Sesn2* + LPS group, suggesting that the inhibition of *Sesn2* significantly decreased the MMP and promoted the cell apoptosis (Fig. 4J). MitoSOX, a mitochondrial superoxide indicator, can not only reflect the level of superoxide in mitochondria but also the level of ROS. The results of fluorescence analysis indicated that the red fluorescence of MitoSOX in the Si-*Sesn2* + LPS group was higher compared with the control + LPS group, indicating that the inhibition of *Sesn2* enhanced ROS levels (Fig. 4K). MitoSOX and MMP are key indicators of mitochondrial activity, suggesting that *Sesn2* may be associated with mitophagy.

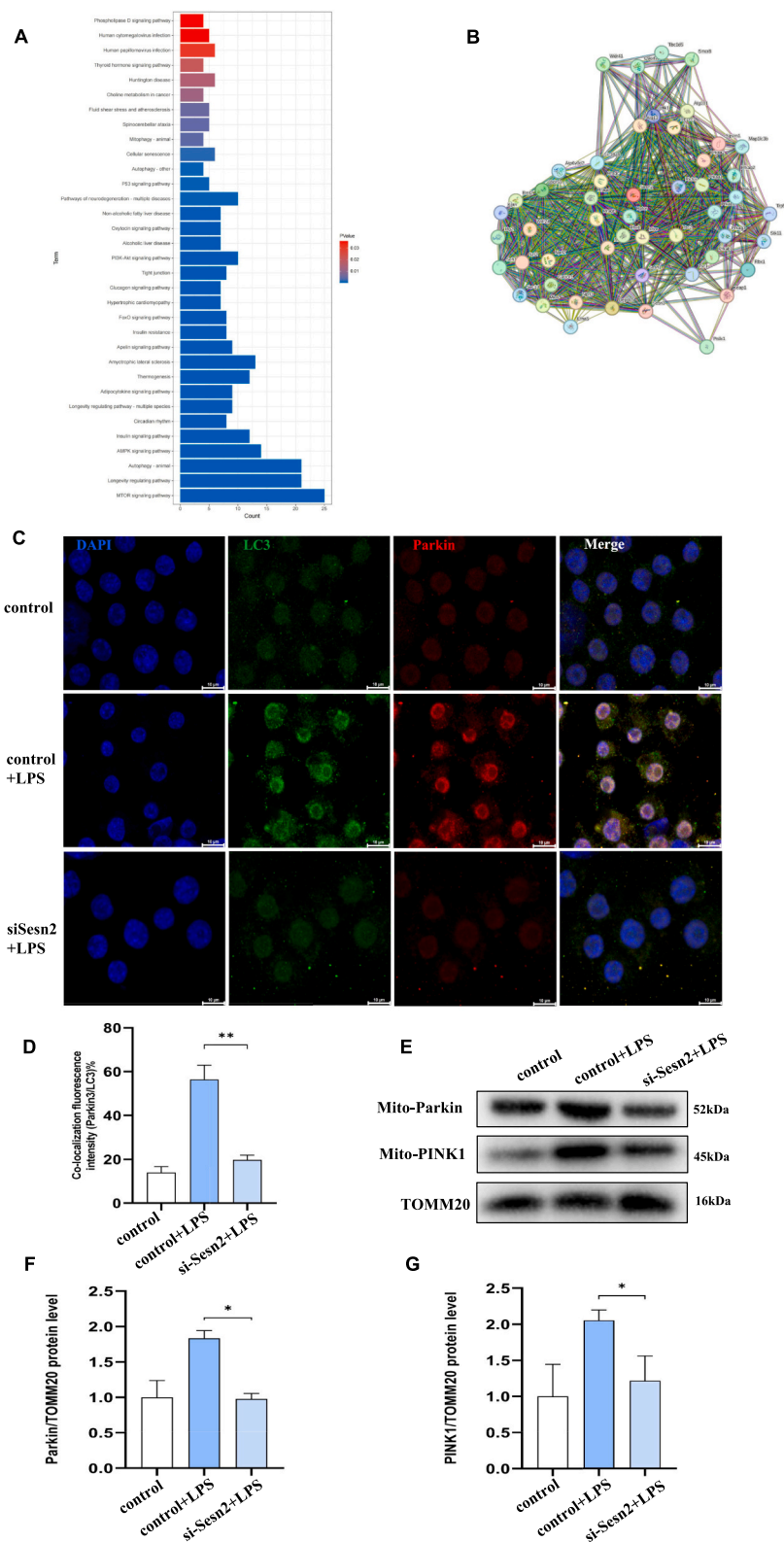
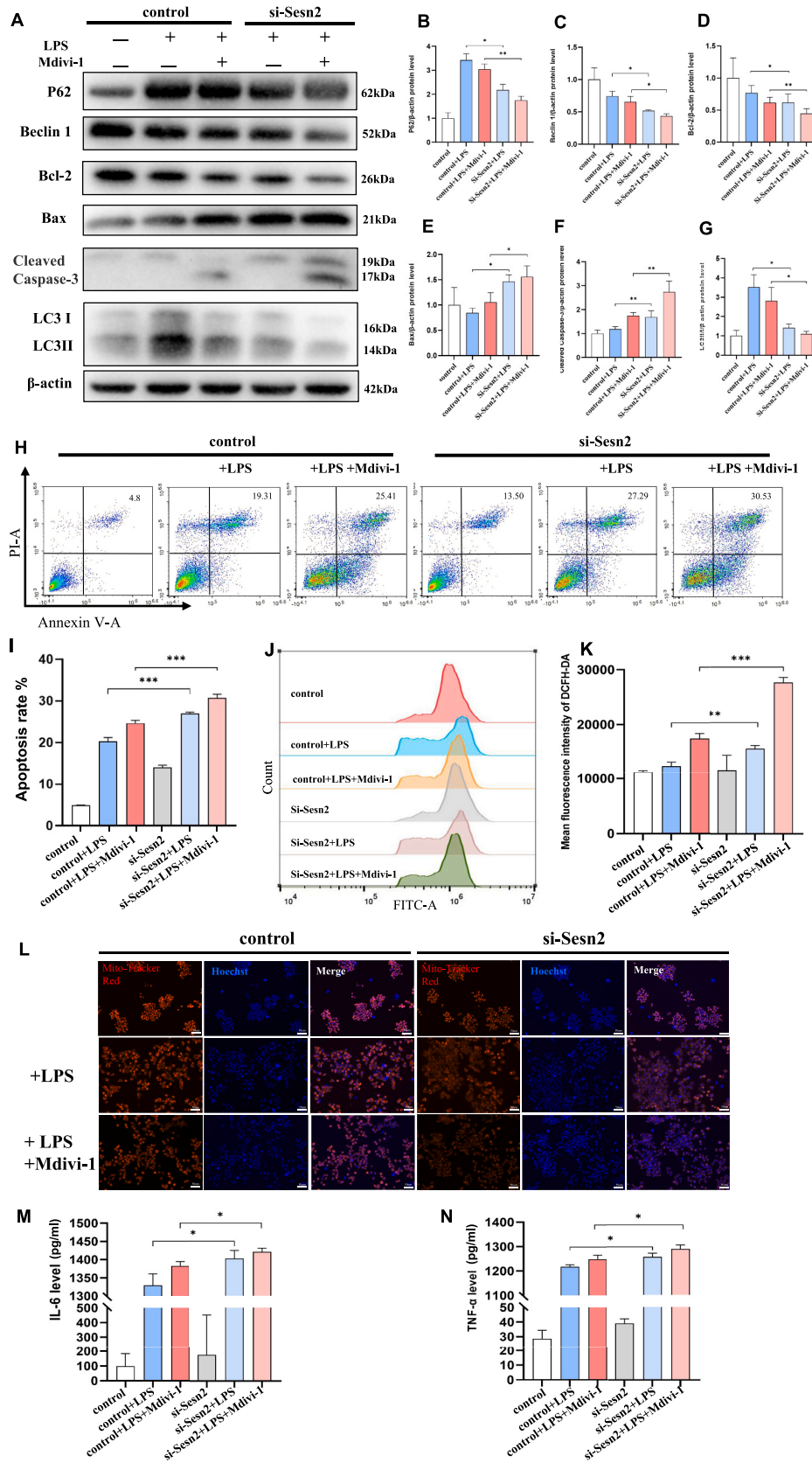


Fig. 5. Inhibition of Sen2 suppresses mitophagy by modulating the PINK1-Parkin pathway in RAW264.7 cells.

A: KEGG pathway for Sen2. **B:** Related proteins interacting with Sen2. **C-D:** Co-localization (C) and mean Co-localization fluorescence intensity analyses (D) of Parkin (red) with LC3 (green) in Si-NC or Si-Sesn2-treated RAW264.7 cells stimulated with 1 $\mu\text{g}/\text{mL}$ LPS for 24 h (Bar = 10 μm). **E-G:** Results of Western blotting (E) and densitometric quantification of Mito-Parkin (F) and Mito-PINK1 (G) mitochondrial proteins in different groups. * $P < 0.05$. KEGG, Kyoto encyclopedia for genes and genomics; LPS, lipopolysaccharide; PINK1, PTEN-induced putative kinase 1. (For interpretation of the references to colour in this figure legend, the reader is referred to the web version of this article.)



(caption on next page)

Fig. 6. Sesn2 improves mitochondrial homeostasis and inflammation levels by decreasing the apoptosis of RAW264.7 cells.

Si-NC or Si-Sesn2-treated RAW264.7 cells were stimulated with 1 $\mu\text{g}/\text{mL}$ LPS alone or LPS + 10 μM Mdivi-1 for 24 h. **A-G:** Results of Western blotting (**A**) and densitometric quantification (**B-G**) of Sqstm1/p62, Beclin1, Bcl-2, Bax, cleaved caspase-3, and LC3II/I in different groups. **H-I:** Flow cytometry (**H**) and mean fluorescence intensity analyses (**I**) were used to detect the rate of apoptosis in each group. **J-K:** Flow cytometry (**J**) and mean fluorescence intensity analyses (**K**) were used to detect ROS in each group. **L:** Immunofluorescence showing the MMP for each group, red fluorescence indicates Mito-Tracker and blue fluorescence indicates Hoechst (Bar = 50 μm). **M-N:** Si-NC or Si-Sesn2-treated RAW264.7 cells and cell supernatants were collected after stimulation with 1 $\mu\text{g}/\text{mL}$ LPS or LPS + 10 μM Mdivi-1 for 24 h. Results of ELISA for IL-6 (**M**) and TNF- α (**N**) levels in different groups. * $P < 0.05$, ** $P < 0.01$, *** $P < 0.001$. ELISA, enzyme-linked immunosorbent assay; LPS, lipopolysaccharide; MMP, mitochondrial membrane potential. (For interpretation of the references to colour in this figure legend, the reader is referred to the web version of this article.)

3.5. Inhibition of Sesn2 suppresses mitophagy by modulating the PINK1-Parkin pathway in RAW264.7 cells

To explore the signaling pathways involving Sesn2, we used the KEGG database to identify statistically different pathways ($P < 0.05$) (Fig. 5A). The analysis revealed that Sesn2 was associated with mitophagy, confirming previous hypotheses. We then searched for the related proteins interacting with Sesn2 using the STRING database and found that these proteins included mitophagy-associated Sqstm1/p62 and LC3 (Fig. 5B). This led us to hypothesize that Sesn2 was involved in mitophagy. Confocal fluorescence imaging revealed that the colocalization of Parkin (a key factor in mitophagy) with LC3 was significantly decreased in the Si-Sesn2 + LPS group compared with the control + LPS group (Fig. 5C, D). To gain further insight into the impact of Sesn2 on mitophagy, we undertook an examination of the expression levels of mitophagy-related proteins in Si-Sesn2 cells. These findings indicated that inhibition of Sesn2 acted negatively on the expression of mitochondrial protein PINK1 and Parkin following LPS treatment (Fig. 5E-G), suggesting that the inhibition of Sesn2 attenuated mitophagy.

3.6. Sesn2 improves mitochondrial homeostasis and inflammation levels by decreasing the apoptosis of RAW264.7 cells

We further employed LPS and a mitophagy inhibitor, Mdivi-1, to demonstrate that a combination of LPS and Mdivi-1 stimulation significantly augmented the levels of cellular Bax and Cleaved caspase3 proteins and led to a decrease in the levels of Sqstm1/p62, Beclin1, Bcl-2 and LC3II/I proteins compared with those stimulated with LPS alone. Similarly, the inhibition of Sesn2 decreased the levels of Sqstm1/p62, Beclin1, Bcl-2, and LC3II/I proteins, while significantly increasing the levels of apoptosis-related proteins Bax and cleaved caspase-3 when stimulated by either LPS alone or a combination of LPS and Mdivi-1 (Fig. 6A-G). We again examined the apoptosis of these six groups of cells using flow cytometry and observed that the inhibition of Sesn2 significantly increased the rate of apoptosis in RAW264.7 cells when stimulated by either LPS alone or a combination of LPS and Mdivi-1 (Fig. 6H, I). Similarly, we also used the fluorescent probe DCFH-DA to determine the ROS levels in each group of cells and observed that the inhibition of Sesn2 increased the degree of ROS in the cells (Fig. 6J, K). To further determine whether Sesn2 is associated with mitophagy, we treated these six groups of cells with MitoTracker Red, a fluorescent probe that specifically labels biologically active mitochondria in cells and detects the MMP. We observed that the reduction of MMP can be achieved by inhibiting Sesn2 (Fig. 6L). To investigate the role of Sesn2 in cellular inflammation and injury induced by LPS or LPS combined with Mdivi-1, we assessed the levels of the pro-inflammatory factors IL-6 and TNF- α in cell culture supernatants. We observed that the inhibition of Sesn2 increased the levels of TNF- α and IL-6 in the supernatants (Fig. 6M, N). These findings suggest that Sesn2 decreases apoptosis, ROS, increases MMP and improves mitochondrial homeostasis.

3.7. Sesn2 promotes macrophage differentiation to the M2 type both in vivo and vitro

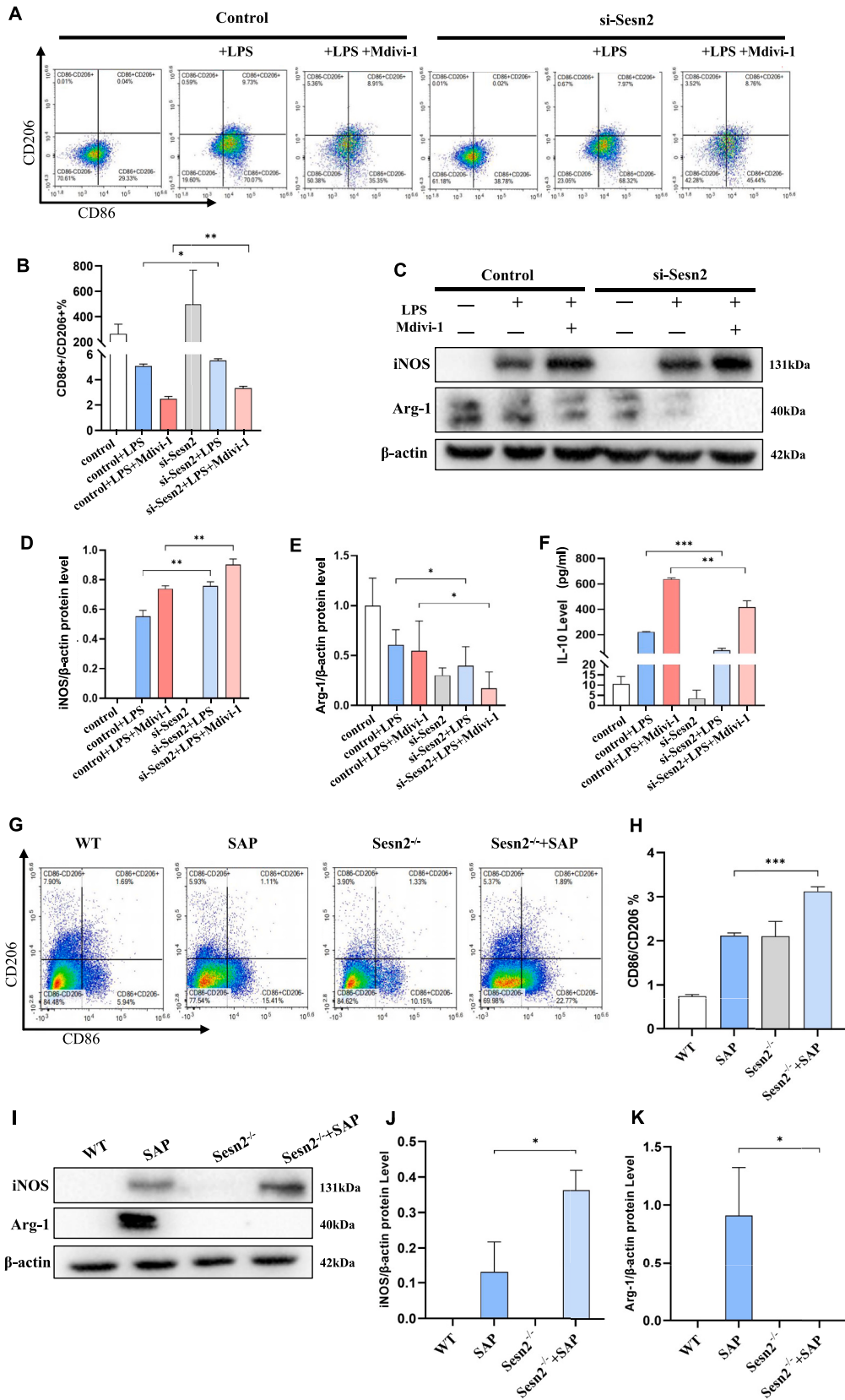
To investigate the role of Sesn2 in macrophage M1/M2 polarization, we determined the CD86/CD206 ratio of RAW264.7 cells using flow

cytometry. As shown in Fig. 7 A and B, treatment with LPS alone or combined with Mdivi-1 significantly decreased the CD86/CD206 ratio. Moreover, the inhibition of Sesn2 further increased the CD86/CD206 ratio, enhanced the expression of M1-tagged CD86, and induced the polarization of macrophages toward the M1 pro-inflammatory phenotype. In the absence of LPS stimulation, iNOS was not expressed in macrophages. WB analysis further confirmed that the inhibition of Sesn2 significantly increased the expression level of the M1 marker iNOS and significantly decreased the expression level of the M2 marker Arg-1 protein when stimulated by either LPS alone or a combination of LPS and Mdivi-1 (Fig. 7C-E). During inflammation, anti-inflammatory factors of IL-10 are mainly secreted by M2 macrophages. The levels of the relevant factors in RAW264.7 cells were determined using ELISA, and the level of IL-10 was observed to significantly decrease after the inhibition of Sesn2 (Fig. 7F). Meanwhile, we extracted primary monocyte macrophages from the spleens of mice and subjected them to flow cytometry. We observed that the CD86/CD206 ratio in the Sesn2^{-/-} + SAP group was significantly higher compared with the SAP group, suggesting that the knockout of Sesn2 promoted the polarization of monocyte macrophages toward the M1 type (Fig. 7G, H). iNOS and Arg-1 were not normally expressed in tissues, but can be induced in tissues after inflammation, infection, or other injury. The results of WB analysis also confirmed this observation, Sesn2^{-/-} + SAP group led to an increase in the expression level of iNOS and a decrease in the expression level of Arg-1 compared with the SAP group (Fig. 7I-K). These results suggest that Sesn2 promotes the polarization of macrophages toward the M2 anti-inflammatory phenotype.

4. Discussion

Most of the current treatments for SAP are conservative and involve nutritional support, fluid management, and antibiotic therapy [4,31,32]. However, our results show that Sesn2 balances mitophagy and apoptosis by regulating the PINK1-Parkin signaling, thereby attenuating pancreatic injury, mitochondrial dysfunction and ROS levels, which is the key role of Sesn2 in regulating the progression of SAP (See Fig. 8).

Sesn2, a stress-inducible protein, can be activated in response to hypoxia, oxidative stress and mitochondrial dysfunction [33]. Despite significant advances in the function of SESN2 in cardiovascular, neurodegenerative, and metabolic diseases [26–28,34], no study has demonstrated the regulatory role of Sesn2 in SAP diseases and its associated mechanisms. Recent studies have revealed that SESN2 plays a crucial role in antioxidants through the Nrf2 pathway [35,36]. Besides, Sesn2 inhibits mTORC1 through AMPK-dependent or independent pathways to maintain organismal homeostasis [37–39]. Sesn2 could also block the production of NADPH-dependent oxidase 4 (nox4)-dependent ROS and peroxynitrite through the activation of AMPK; thus, preventing the subsequent uncoupling of endothelial nitric oxide synthase and eventually restoring NO levels and attenuating glomerular fibrosis [40]. We observed that the knockout of Sesn2 aggravated damage to the pancreas and other organs in SAP mice. It also increased the level of α -AMY (a diagnostic indicator of SAP). Moreover, Sesn2-knockout SAP mice showed the most severe pancreatic mitochondrial damage, with a significant reduction in both autophagosomes and mitochondrial autophagosomes compared with SAP mice. WB and IHC assays demonstrated



(caption on next page)

Fig. 7. Sesn2 promotes macrophage differentiation to the M2 type both in vivo and in vitro.

Si-NC or Si-Sesn2-treated RAW264.7 cells were stimulated with 1 $\mu\text{g}/\text{mL}$ LPS alone or LPS + 10 μM Mdivi-1 for 24 h. **A-B:** Flow cytometry (**A**) and CD86/CD206 ratio analyses (**B**) were used to detect the polarization of RAW264.7 cells in each group. **C-E:** Results of Western blotting (**C**) and densitometric quantification of iNOS (**D**) and Arg-1 (**E**) of RAW264.7 cells in different groups. **F:** Results of ELISA for the level of IL-10 in different groups. Wild-type and Sesn2^{-/-} mice were injected with CAE and LPS (n = 6/group). **G-H:** Flow cytometry (**G**) and CD86/CD206 ratio analyses (**H**) were used to detect the polarization of mouse primary monocyte macrophages in each group. **I-K:** Results of Western blotting (**I**) and densitometric quantification of iNOS (**J**) and Arg-1 (**K**) in the mouse pancreatic tissue from different groups. * $P < 0.05$, ** $P < 0.01$, *** $P < 0.001$. CAE, ceruletide; LPS, lipopolysaccharide.

that Sesn2 promoted the expression of mitophagy-related proteins PINK1 and Parkin and increased the co-localization of LC3 and the mitochondrial marker TOMM20, suggesting that it attenuates SAP injury through mitophagy. We also found that Sesn2 reduced the level of the pro-inflammatory factor IL-6 and decreased the rate of apoptosis in mouse primary monocyte macrophages. Thus, our findings suggest that Sesn2 eliminates damaged mitochondria through mitophagy and reduces apoptosis as a key factor in alleviating SAP injury.

Macrophages represent the most abundant immune cells within the pancreas in the early stages of SAP and are involved in the inflammatory response of SAP. They play a pivotal role in inflammatory response associated with SAP. The rapid activation of macrophages is attributed to the presence of a multitude of pancreatic enzymes and cytokines; These macrophages are associated with inflammation from local to systemic development of SAP [41,42]. Moreover, several studies have described the autophagy-stimulating anti-apoptotic effects of Sesn2 in various cell types [27,43,44]. For example, Song et al. [45] showed that the overexpression of Sesn2 inhibited apoptosis and oxidative stress and ameliorated podocyte injury. In this study, we observed that the expression of Sesn2 was significantly increased after the stimulation of RAW264.7 cells with LPS. Following stimulation with LPS both in vivo and in vitro, Sesn2 increased the MMP and expression of autophagy-related proteins and also decreased the level of ROS and expression of apoptosis-related proteins. When Mdivi-1 was added to LPS, Sesn2 further increased the expression of anti-apoptosis-related proteins and autophagy related proteins. Flow cytometry also revealed that Sesn2 reduced the rate of apoptosis of RAW264.7 cells and mouse primary mononuclear macrophage. Moreover, Sesn2 decreased the expression of

the pro-inflammatory factors TNF- α and IL-6 in cell supernatants or mouse sera. These findings suggest that Sesn2 may play a major role in the inhibition of macrophages apoptosis and inflammation, elimination of ROS, and increase of autophagy.

Interestingly, we found that Sesn2 was involved in mitophagy through the PINK1-Parkin pathway to reduce apoptosis. When mitochondria encounter a lack of nutrients, increased ROS, or cellular aging, a gradual increase in the number of mitochondrial DNA mutations, damaged mitochondrial depolarization, and loss of MMP will occur [46,47]. To maintain homeostasis in the mitochondria and cells, the cell undergoes the selective wrapping of the damaged mitochondria to form mitochondrial autophagosomes, which are then fused with lysosomes, and these damaged mitochondria are degraded in a process called mitophagy [48,49]. Mitophagy plays a key role in maintaining a balance between the number of healthy and damaged mitochondria in cells [50,51]. Our findings demonstrate that Sesn2 restores the MMP that was reduced after LPS stimulation. Moreover, Sesn2 decreases the level of MitoSOX, suggesting that it may play an important role in scavenging the damaged mitochondria. Recently, it has been shown that under stressful conditions such as the process of muscle formation, Sesn2 can regulate ROS-induced mitochondrial quality control [52]. Data from Liu et al. [53] showed that sarcopenia led to an increase in dysfunctional mitochondria and the knockdown of Sesn2 led to an imbalance of mitochondrial fusion and fission, an increase in mitochondrial biogenesis, and damage to mitophagy both in vivo and in vitro. Moreover, we used the KEGG database to demonstrate that Sesn2 may be involved in mitophagy. We also confirmed that Sesn2 increased mitophagy through the PINK1-Parkin pathway, as well as increased the expression of anti-

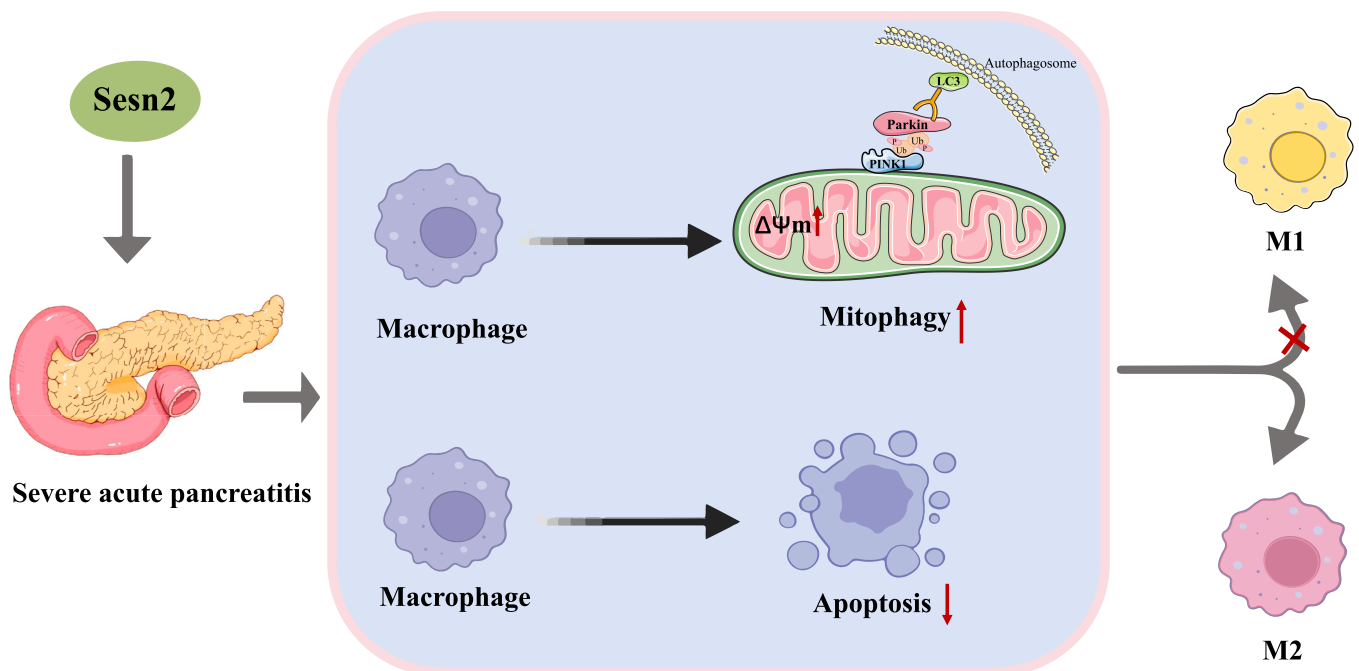


Fig. 8. Upregulation of Sesn2 alleviates the progression of SAP by mediating mitophagy through the PINK1-Parkin pathway and reducing apoptosis.

Upregulation of Sesn2 stimulated PINK1 at the outer mitochondrial membrane and recruited Parkin to activate mitophagy and remove the damaged mitochondria, thereby attenuating apoptosis and delaying the progression of SAP.

P:phosphorylation; Ub: ubiquitin.

apoptosis-related proteins in RAW264.7 cells and SAP mouse model by using WB assays and fluorescence co-localization. Here, we observed that the expression of mitophagy-related proteins PINK1 and Parkin was significantly decreased in the pancreas of SAP mice when knockout of *Sesn2*, which suggested that *Sesn2* was involved in the regulation of mitophagy and mitochondrial damage in SAP. Furthermore, the results of electron microscopy also showed the mitochondria in the pancreas of *Sesn2*^{-/-} + SAP mice were swelling with extensive mitochondrial cristae dissolution and few autolysosomes autophagosomes and mitochondrial autophagosomes. Therefore, besides its antioxidant, mTOR-inhibitory, and anti-apoptotic effects, *Sesn2* may also play a role in balancing mitophagy and apoptotic. Thus, *Sesn2* reduces apoptosis by removing dysfunctional mitochondria through PINK1-dependent mitophagy, providing new insights into the regulation of cellular homeostasis.

Macrophages play an important role in maintaining the homeostatic balance in the body and resisting invading pathogens. When the environment changes, macrophages polarize into different subtypes, namely, M1 macrophage and M2 macrophage [54–56]. The altered expression of cell surface markers indicates macrophage polarization. CD80, CD86, and CD16/32, as well as the pro-inflammatory factors TNF- α , IL-12 and IL-6, are elevated in M1 macrophages. In contrast, M2 macrophages overexpress CD206 and mannose receptor arginase-1 (Arg-1), which secretes the anti-inflammatory factor IL-10 [57–60]. Thus, understanding the alterations in macrophage polarization can help modify cellular phenotypes using specific drugs to treat disease [61]. A study verified the link between *Sesn2* and microglia polarization, demonstrating that *Sesn2* inhibited microglia polarization in M1 macrophages and promoted it in M2 macrophages; thus, exhibiting neuroprotective effects [62]. To our knowledge, no study has validated the relationship between *Sesn2* and macrophage polarization in the SAP model. Our study demonstrated that *Sesn2* decreased the CD86/CD206 ratio, increased the expression of the M2 phenotype marker Arg-1, and decreased the expression of the M1 phenotype marker iNOS, both in RAW264.7 cells and primary monocyte macrophages from SAP mice.

5. Conclusions

In summary, we confirmed that *Sesn2* balances apoptosis and mitophagy by regulating the PINK1-Parkin signaling, thereby attenuating pancreatic injury, inflammation levels and ameliorating mitochondrial dysfunction. In addition, *Sesn2* increased cellular MMP, decreased ROS levels and promoted macrophage toward an M2 anti-inflammatory phenotype, improving mitochondrial homeostasis by promoting mitophagy and reducing apoptosis. Despite the current unavailability of *Sesn2* agonists or inhibitors, we have demonstrated a potential therapeutic strategy for SAP. The findings elucidate the regulatory impact of the *Sesn2* and PINK1-Parkin pathway on cell fate, which may be a pivotal factor in directing the progression of apoptosis and mitophagy in the context of SAP.

Author contribution

Yuxi Yang conceived the study and designed the experiments. Yuxi Yang, Yiqiu Peng, Yingying Li, Tingjuan Shi and Ning Xu performed the experiments and analyzed the data. Yingyi Luan and Chenghong Yin substantively revised the manuscript.

Availability of data and materials

All data generated during this study are included either in this article or in Additional files.

Ethics approval

All experimental procedures involving animals were conducted in

accordance with the Basel Declaration and were approved by the Ethics Committee for Laboratory Animals of the Beijing Obstetrics and Gynecology Hospital, Capital Medical University (No. BOGH21–2305-7, approval date April 26,2023).

Consent for publication

Not applicable.

Availability of data and materials

The data sets supporting the conclusions of this article are included within the article.

Funding

This work was supported by Leading Talents in the Construction Project of High Level Public Health Technical Talents in Beijing (Np.2022–1–003).

Authors' information.

Yingyi Luan, E-mail: luanyingyi@mail.ccmu.edu.cn

Chenghong Yin, E-mail: yinhh@ccmu.edu.cn;

CRediT authorship contribution statement

Yuxi Yang: Writing – original draft, Methodology, Conceptualization. **Yiqiu Peng:** Formal analysis. **Yingying Li:** Formal analysis. **Tingjuan Shi:** Data curation. **Ning Xu:** Data curation. **Yingyi Luan:** Writing – review & editing, Supervision, Methodology. **Chenghong Yin:** Writing – review & editing, Methodology, Funding acquisition.

Declaration of competing interest

The authors declare that they have no known competing financial interests or personal relationships that could have appeared to influence the work reported in this paper.

Data availability

Data will be made available on request.

Acknowledgements

No Acknowledgement.

Appendix A. Supplementary data

Supplementary data to this article can be found online at <https://doi.org/10.1016/j.cellsig.2024.111518>.

References

- [1] P. Szatmary, T. Grammatikopoulos, W. Cai, W. Huang, R. Mukherjee, C. Halloran, G. Beyer, R. Sutton, Acute pancreatitis: diagnosis and treatment, *Drugs* 82 (2022) 1251–1276, <https://doi.org/10.1007/s40265-022-01766-4>.
- [2] P.K. Garg, V.P. Singh, Organ failure due to systemic injury in acute pancreatitis, *Gastroenterology* 156 (2019) 2008–2023, <https://doi.org/10.1053/j.gastro.2018.12.041>.
- [3] M.S. Petrov, D. Yadav, Global epidemiology and holistic prevention of pancreatitis, *Nat. Rev. Gastroenterol. Hepatol.* 16 (2019) 175–184, <https://doi.org/10.1038/s41575-018-0087-5>.
- [4] E. Zerem, A. Kurtcehajic, S. Kunosić, D. Zerem Malkoćević, O. Zerem, Current trends in acute pancreatitis: diagnostic and therapeutic challenges, *World J. Gastroenterol.* 29 (2023) 2747–2763, <https://doi.org/10.3748/wjg.v29.i18.2747>.
- [5] L. Zhang, J. Shi, D. Du, N. Niu, S. Liu, X. Yang, P. Lu, X. Shen, N. Shi, L. Yao, R. Zhang, G. Hu, G. Lu, Q. Zhu, T. Zeng, T. Liu, Q. Xia, W. Huang, J. Xue, Ketogenesis acts as an endogenous protective programme to restrain inflammatory macrophage activation during acute pancreatitis, *EBioMedicine* 78 (2022) 103959, <https://doi.org/10.1016/j.ebiom.2022.103959>.
- [6] Q. Hu, J. Yao, X. Wu, J. Li, G. Li, W. Tang, J. Liu, M. Wan, Emodin attenuates severe acute pancreatitis-associated acute lung injury by suppressing pancreatic exosome-mediated alveolar macrophage activation, *Acta Pharm. Sin.* B 12 (2022) 3986–4003, <https://doi.org/10.1016/j.apsb.2021.10.008>.

- [7] P. Bernardi, A. Rasola, M. Forte, G. Lippe, The mitochondrial permeability transition pore: channel formation by F-ATP synthase, integration in signal transduction, and role in pathophysiology, *Physiol. Rev.* 95 (2015) 1111–1155, <https://doi.org/10.1152/physrev.00001.2015>.
- [8] A. Habtezion, A.S. Gukovskaya, S.J. Pandol, Acute pancreatitis: a multifaceted set of organelle and cellular interactions, *Gastroenterology* 156 (2019) 1941–1950, <https://doi.org/10.1053/j.gastro.2018.11.082>.
- [9] P.A. Banks, T.L. Bollen, C. Dervenis, H.G. Gooszen, C.D. Johnson, M.G. Sarr, G. G. Tsiotos, S.S. Vege, Classification of acute pancreatitis—2012: revision of the Atlanta classification and definitions by international consensus, *Gut* 62 (2013) 102–111, <https://doi.org/10.1136/gutjnl-2012-302779>.
- [10] J. Maléth, P. Hegyi, Ca²⁺ toxicity and mitochondrial damage in acute pancreatitis: translational overview, *Philos. Trans. R. Soc. Lond. Ser. B Biol. Sci.* 371 (2016), <https://doi.org/10.1098/rstb.2015.0425>.
- [11] G. Biczó, E.T. Vegh, N. Shalbuva, O.A. Mareninova, J. Elperin, E. Lotshaw, S. Gretler, A. Lugea, S.R. Malla, D. Dawson, P. Ruchala, J. Whitelegge, S.W. French, L. Wen, S.Z. Husain, F.S. Gorelick, P. Hegyi, Z. Rakonczay Jr., I. Gukovsky, A. S. Gukovskaya, Mitochondrial dysfunction, through impaired autophagy, leads to endoplasmic reticulum stress, deregulated lipid metabolism, and pancreatitis in animal models, *Gastroenterology* 154 (2018) 689–703, <https://doi.org/10.1053/j.gastro.2017.10.012>.
- [12] X. Yu, C. Dai, X. Zhao, Q. Huang, X. He, R. Zhang, Z. Lin, Y. Shen, Ruthenium red attenuates acute pancreatitis by inhibiting MCU and improving mitochondrial function, *Biochem. Biophys. Res. Commun.* 635 (2022) 236–243, <https://doi.org/10.1016/j.bbrc.2022.10.044>.
- [13] B. Jabłońska, S. Mrowiec, Nutritional support in patients with severe acute pancreatitis-current standards, *Nutrients* 13 (2021), <https://doi.org/10.3390/nu13051498>.
- [14] M.A. Mederos, H.A. Reber, M.D. Giris, Acute pancreatitis: a review, *Jama* 325 (2021) 382–390, <https://doi.org/10.1001/jama.2020.20317>.
- [15] E. Zerem, Treatment of severe acute pancreatitis and its complications, *World J. Gastroenterol.* 20 (2014) 13879–13892, <https://doi.org/10.3748/wjg.v20.i38.13879>.
- [16] Y. Lu, Z. Li, S. Zhang, T. Zhang, Y. Liu, L. Zhang, Cellular mitophagy: mechanism, roles in diseases and small molecule pharmacological regulation, *Theranostics* 13 (2023) 736–766, <https://doi.org/10.7150/thno.79876>.
- [17] T. Zhang, Q. Liu, W. Gao, S.A. Sehgal, H. Wu, The multifaceted regulation of mitophagy by endogenous metabolites, *Autophagy* 18 (2022) 1216–1239, <https://doi.org/10.1080/15548627.2021.1975914>.
- [18] M. Onishi, K. Yamano, M. Sato, N. Matsuda, K. Okamoto, Molecular mechanisms and physiological functions of mitophagy, *EMBO J.* 40 (2021) e104705, <https://doi.org/10.15252/embj.2020104705>.
- [19] J. Yao, J. Wang, Y. Xu, Q. Guo, Y. Sun, J. Liu, S. Li, Y. Guo, L. Wei, CDK9 inhibition blocks the initiation of PINK1-PRKN-mediated mitophagy by regulating the SIRT1-FOXO3-BNIP3 axis and enhances the therapeutic effects involving mitochondrial dysfunction in hepatocellular carcinoma, *Autophagy* 18 (2022) 1879–1897, <https://doi.org/10.1080/15548627.2021.2007027>.
- [20] X.Q. Xie, Y. Yang, Q. Wang, H.F. Liu, X.Y. Fang, C.L. Li, Y.Z. Jiang, S. Wang, H. Y. Zhao, J.Y. Miao, S.S. Ding, X.D. Liu, X.H. Yao, W.T. Yang, J. Jiang, Z.M. Shao, G. Jin, X.W. Bian, Targeting ATAD3A-PINK1-mitophagy axis overcomes chemioimmunotherapy resistance by redirecting PD-L1 to mitochondria, *Cell Res.* 33 (2023) 215–228, <https://doi.org/10.1038/s41422-022-00766-z>.
- [21] G. Lou, K. Palikaras, S. Lautrup, M. Scheibye-Knudsen, N. Tavernarakis, E.F. Fang, Mitophagy and neuroprotection, *Trends Mol. Med.* 26 (2020) 8–20, <https://doi.org/10.1016/j.molmed.2019.07.002>.
- [22] A.S. Titus, E.A. Sung, D. Zablocki, J. Sadoshima, Mitophagy for cardioprotection, *Basic Res. Cardiol.* 118 (2023) 42, <https://doi.org/10.1007/s00395-023-01009-x>.
- [23] L.X. Wang, X.M. Zhu, Y.M. Yao, Sestrin2: Its Potential Role and Regulatory Mechanism in Host Immune Response in Diseases, *Front. Immunol.* 10 (2019) 2797, <https://doi.org/10.3389/fimmu.2019.02797>.
- [24] S.D. Chen, J.L. Yang, Y.H. Hsieh, T.K. Lin, Y.C. Lin, A.C. Chao, D.I. Yang, Potential roles of Sestrin2 in Alzheimer's disease: Antioxidation, autophagy promotion, and beyond, *Biomedicines* 9 (2021), <https://doi.org/10.3390/biomedicines9101308>.
- [25] L. Gong, Z. Wang, Z. Wang, Z. Zhang, Sestrin2 as a potential target for regulating metabolic-related diseases, *Front Endocrinol (Lausanne)*. 12 (2021) 751020, <https://doi.org/10.3389/fendo.2021.751020>.
- [26] Z. Tian, B.J. Yan, W. Luo, D.D. Gui, K. Zhou, K.J. Tian, Y. Ma, Z.X. Zhou, Z.S. Jiang, Sestrin2 in atherosclerosis, *Chin. Chim. Acta* 523 (2021) 325–329, <https://doi.org/10.1016/j.cca.2021.10.019>.
- [27] D. Han, H. Kim, S. Kim, Q.A. Le, S.Y. Han, J. Bae, H.W. Shin, H.G. Kang, K.H. Han, J. Shin, H.W. Park, Sestrin2 protects against cholestatic liver injury by inhibiting endoplasmic reticulum stress and NLRP3 inflammasome-mediated pyroptosis, *Exp. Mol. Med.* 54 (2022) 239–251, <https://doi.org/10.1038/s12276-022-00737-9>.
- [28] X. Che, J. Chai, Y. Fang, X. Zhang, A. Zu, L. Li, S. Sun, W. Yang, Sestrin2 in hypoxia and hypoxia-related diseases, *Redox Rep.* 26 (2021) 111–116, <https://doi.org/10.1080/13510002.2021.1948774>.
- [29] H.J. Hu, Z.Y. Shi, X.L. Lin, S.M. Chen, Q.Y. Wang, S.Y. Tang, Upregulation of Sestrin2 expression protects against macrophage apoptosis induced by oxidized low-density lipoprotein, *DNA Cell Biol.* 34 (2015) 296–302, <https://doi.org/10.1089/dna.2014.2627>.
- [30] X. Yuan, J. Wu, X. Guo, W. Li, C. Luo, S. Li, B. Wang, L. Tang, H. Sun, Autophagy in acute pancreatitis: organelle interaction and microRNA regulation, *Oxidative Med. Cell. Longev.* 2021 (2021) 8811935, <https://doi.org/10.1155/2021/8811935>.
- [31] E. de Madaria, J.L. Buxbaum, P. Maisonneuve, A. García García de Paredes, P. Zapater, L. Guilbert, A. Vaillou-Rocamora, M. Rodríguez-Gandía, J. Donate-Ortega, E.E. Lozada-Hernández, Collazo Moreno AJR, A. Lira-Aguilar, L.P. Llovet, R. Mehta, R. Tandel, P. Navarro, A.M. Sánchez-Pardo, C. Sánchez-Marin, M. Corderos, I. Fernández-Cabrera, F. Casals-Seoane, D. Casas Deza, E. Lauret-Braña, E. Martí-Marqués, L.M. Camacho-Montano, V. Ubieto, M. Ganuza, F. Bolado, Aggressive or Moderate Fluid Resuscitation in Acute Pancreatitis, *N. Engl. J. Med.* 387 (2022) 989–1000, <https://doi.org/10.1056/NEJMoa2202884>.
- [32] R. Pezzilli, A. Zerbi, D. Campra, G. Capurso, R. Golfieri, P.G. Arcidiacono, P. Billi, G. Butturini, L. Calculli, R. Cannizzaro, S. Carrara, S. Crippa, R. De Gaudio, P. De Rai, L. Frulloni, E. Mazza, M. Mutignani, N. Pagano, P. Rabitti, G. Balzano, Consensus guidelines on severe acute pancreatitis, *Dig. Liver Dis.* 47 (2015) 532–543, <https://doi.org/10.1016/j.dld.2015.03.022>.
- [33] X. Wang, J. Yang, H. Li, H. Mu, L. Zeng, S. Cai, P. Su, H. Li, L. Zhang, W. Xiang, miR-484 mediates oxidative stress-induced ovarian dysfunction and promotes granulosa cell apoptosis via SESN2 downregulation, *Redox Biol.* 62 (2023) 102684, <https://doi.org/10.1016/j.redox.2023.102684>.
- [34] J. Sun, F.H. Song, J.Y. Wu, L.Q. Zhang, D.Y. Li, S.J. Gao, D.Q. Liu, Y.Q. Zhou, W. Mei, Sestrin2 overexpression attenuates osteoarthritis pain via induction of AMPK/PGC-1 α -mediated mitochondrial biogenesis and suppression of neuroinflammation, *Brain Behav. Immun.* 102 (2022) 53–70, <https://doi.org/10.1016/j.bbi.2022.02.015>.
- [35] X. Han, C. Ding, G. Zhang, R. Pan, Y. Liu, N. Huang, N. Hou, F. Han, W. Xu, X. Sun, Liraglutide ameliorates obesity-related nonalcoholic fatty liver disease by regulating Sestrin2-mediated Nrf2/HO-1 pathway, *Biochem. Biophys. Res. Commun.* 525 (2020) 895–901, <https://doi.org/10.1016/j.bbrc.2020.03.032>.
- [36] J. Tian, X. Wang, H. Shi, H. Wu, C. Wang, N. Liu, L. Guan, Z. Zhang, Sestrin2/Keap1/Nrf2 pathway regulates mucus hypersecretion in pulmonary epithelium induced by traffic-related PM_{2.5} and water-soluble extracts, *Ecotoxicol. Environ. Saf.* 264 (2023) 115455, <https://doi.org/10.1016/j.ecoenv.2023.115455>.
- [37] A.V. Budanov, M. Karin, p53 target genes sestrin1 and sestrin2 connect genotoxic stress and mTOR signaling, *Cell* 134 (2008) 451–460, <https://doi.org/10.1016/j.cell.2008.06.028>.
- [38] J.H. Lee, A.V. Budanov, S. Talukdar, E.J. Park, H.L. Park, H.W. Park, G. Bandyopadhyay, N. Li, M. Aghajan, I. Jang, A.M. Wolfe, G.A. Perkins, M. H. Ellisman, E. Bier, M. Scadeng, M. Foretz, B. Viollet, J. Olefsky, M. Karin, Maintenance of metabolic homeostasis by Sestrin2 and Sestrin3, *Cell Metab.* 16 (2012) 311–321, <https://doi.org/10.1016/j.cmet.2012.08.004>.
- [39] Y. Ma, G. Zhang, Z. Kuang, Q. Xu, T. Ye, X. Li, N. Qu, F. Han, C. Kan, X. Sun, Empagliflozin activates Sestrin2-mediated AMPK/mTOR pathway and ameliorates lipid accumulation in obesity-related nonalcoholic fatty liver disease, *Front. Pharmacol.* 13 (2022) 944886, <https://doi.org/10.3389/fphar.2022.944886>.
- [40] A.A. Eid, D.Y. Lee, L.J. Roman, K. Khazim, Y. Gorin, Sestrin 2 and AMPK connect hyperglycemia to Nox4-dependent endothelial nitric oxide synthase uncoupling and matrix protein expression, *Mol. Cell. Biol.* 33 (2013) 3439–3460, <https://doi.org/10.1128/mcb.00217-13>.
- [41] F. Duan, X. Wang, H. Wang, Y. Wang, Y. Zhang, J. Chen, X. Zhu, B. Chen, GDF11 ameliorates severe acute pancreatitis through modulating macrophage M1 and M2 polarization by targeting the TGF β 1/SMAD-2 pathway, *Int. Immunopharmacol.* 108 (2022) 108777, <https://doi.org/10.1016/j.intimp.2022.108777>.
- [42] T. Lin, M. Peng, Q. Zhu, X. Pan, S1PR2 participates in intestinal injury in severe acute pancreatitis by regulating macrophage pyroptosis, *Front. Immunol.* 15 (2024) 1405622, <https://doi.org/10.3389/fimmu.2024.1405622>.
- [43] N. Qu, J. Qu, N. Huang, K. Zhang, T. Ye, J. Shi, B. Chen, C. Kan, J. Zhang, F. Han, N. Hou, X. Sun, R. Pan, Calycosin induces autophagy and apoptosis via Sestrin2/AMPK/mTOR in human papillary thyroid cancer cells, *Front. Pharmacol.* 13 (2022) 1056687, <https://doi.org/10.3389/fphar.2022.1056687>.
- [44] S. Lee, J. Shin, Y. Hong, S.M. Shin, H.W. Shin, J. Shin, S.K. Lee, H.W. Park, Sestrin2 alleviates palmitate-induced endoplasmic reticulum stress, apoptosis, and defective invasion of human trophoblast cells, *Am. J. Reprod. Immunol.* 83 (2020) e13222, <https://doi.org/10.1111/aji.13222>.
- [45] S. Song, C. Shi, Y. Bian, Z. Yang, L. Mu, H. Wu, H. Duan, Y. Shi, Sestrin2 remedies podocyte injury via orchestrating TSP-1/TGF- β 1/Smad3 axis in diabetic kidney disease, *Cell Death Dis.* 13 (2022) 663, <https://doi.org/10.1038/s41419-022-05120-0>.
- [46] L. Doblado, C. Lueck, C. Rey, A.K. Samhan-Arias, I. Prieto, A. Stacchiotti, M. Monsalvo, Mitophagy in human diseases, *Int. J. Mol. Sci.* 22 (2021), <https://doi.org/10.3390/ijms22083903>.
- [47] X. Zhang, M.D. Lee, C. Buckley, C. Wilson, J.G. McCarron, Mitochondria regulate TRPV4-mediated release of ATP, *Br. J. Pharmacol.* 179 (2022) 1017–1032, <https://doi.org/10.1111/bph.15687>.
- [48] J. Guo, W.C. Chiang, Mitophagy in aging and longevity, *IUBMB Life* 74 (2022) 296–316, <https://doi.org/10.1002/iub.2585>.
- [49] Z. Shan, W.H. Fa, C.R. Tian, C.S. Yuan, N. Jie, Mitophagy and mitochondrial dynamics in type 2 diabetes mellitus treatment, *Aging (Albany NY)* 14 (2022) 2902–2919, <https://doi.org/10.18632/aging.203969>.
- [50] C. Ploumi, I. Daskalaki, N. Tavernarakis, Mitochondrial biogenesis and clearance: a balancing act, *FEBS J.* 284 (2017) 183–195, <https://doi.org/10.1111/febs.13820>.
- [51] L. Su, J. Zhang, H. Gomez, J.A. Kellum, Z. Peng, Mitochondria ROS and mitophagy in acute kidney injury, *Autophagy* 19 (2023) 401–414, <https://doi.org/10.1080/15548627.2022.2084862>.
- [52] L.F. Piochii, I.F. Machado, C.M. Palmeira, A.P. Rolo, Sestrin2 and mitochondrial quality control: potential impact in myogenic differentiation, *Ageing Res. Rev.* 67 (2021) 101309, <https://doi.org/10.1016/j.arr.2021.101309>.
- [53] S. Liu, C. Yu, L. Xie, Y. Niu, L. Fu, Aerobic exercise improves mitochondrial function in sarcopenia mice through Sestrin2 in an AMPK α 2-dependent manner, *J. Gerontol. A Biol. Sci. Med. Sci.* 76 (2021) 1161–1168, <https://doi.org/10.1093/geronl/glab029>.

- [54] L.C. Davies, S.J. Jenkins, J.E. Allen, P.R. Taylor, Tissue-resident macrophages, *Nat. Immunol.* 14 (2013) 986–995, <https://doi.org/10.1038/ni.2705>.
- [55] C. Yunna, H. Mengru, W. Lei, C. Weidong, Macrophage M1/M2 polarization, *Eur. J. Pharmacol.* 877 (2020) 173090, <https://doi.org/10.1016/j.ejphar.2020.173090>.
- [56] M. Genin, F. Clement, A. Fattaccioli, M. Raes, C. Michiels, M1 and M2 macrophages derived from THP-1 cells differentially modulate the response of cancer cells to etoposide, *BMC Cancer* 15 (2015) 577, <https://doi.org/10.1186/s12885-015-1546-9>.
- [57] X. Chen, Y. Liu, Y. Gao, S. Shou, Y. Chai, The roles of macrophage polarization in the host immune response to sepsis, *Int. Immunopharmacol.* 96 (2021) 107791, <https://doi.org/10.1016/j.intimp.2021.107791>.
- [58] G.R. Gunassekaran, S.M. Poongkavithai Vadevoo, M.C. Baek, B. Lee, M1 macrophage exosomes engineered to foster M1 polarization and target the IL-4 receptor inhibit tumor growth by reprogramming tumor-associated macrophages into M1-like macrophages, *Biomaterials* 278 (2021) 121137, <https://doi.org/10.1016/j.biomaterials.2021.121137>.
- [59] M. Liu, X. Meng, Z. Xuan, S. Chen, J. Wang, Z. Chen, J. Wang, X. Jia, Effect of Er Miao san on peritoneal macrophage polarisation through the miRNA-33/NLRP3 signalling pathway in a rat model of adjuvant arthritis, *Pharm. Biol.* 60 (2022) 846–853, <https://doi.org/10.1080/13880209.2022.2066700>.
- [60] T. Dong, X. Chen, H. Xu, Y. Song, H. Wang, Y. Gao, J. Wang, R. Du, H. Lou, T. Dong, Mitochondrial metabolism mediated macrophage polarization in chronic lung diseases, *Pharmacol. Ther.* 239 (2022) 108208, <https://doi.org/10.1016/j.pharmthera.2022.108208>.
- [61] K. Yang, C. Xu, Y. Zhang, S. He, D. Li, Sestrin2 suppresses classically activated macrophages-mediated inflammatory response in myocardial infarction through inhibition of mTORC1 signaling, *Front. Immunol.* 8 (2017) 728, <https://doi.org/10.3389/fimmu.2017.00728>.
- [62] T. He, W. Li, Y. Song, Z. Li, Y. Tang, Z. Zhang, G.Y. Yang, Sestrin2 regulates microglia polarization through mTOR-mediated autophagic flux to attenuate inflammation during experimental brain ischemia, *J. Neuroinflammation* 17 (2020) 329, <https://doi.org/10.1186/s12974-020-01987-y>.